J. Membrane Biol. 119, 253–265 (1991)
0022263191000248

The Journal of
Membrane Biology

Developmental Changes in Regulation of Embryonic Chick Heart Gap Junctions

Richard D. Veenstra
Department of Pharmacology, State University of New York/Health Science Center at Syracuse, Syracuse, New York 13210

Summary. Embryonic chick myocyte pairs were isolated from ventricular tissue of 4-day, 14-day, and 18-day heart for the purpose of examining the relationship between macroscopic junctional conductance and transjunctional voltage during cardiac development. The double whole-cell patch-clamp technique was employed to directly measure junctional conductance over a transjunctional voltage range of ±100 mV. At all ages, the instantaneous junctional current (or conductance = current/voltage) varied linearly with respect to transjunctional voltage. This initial response was followed by a time- and voltage-dependent decline in junctional current to new steady-state values. For every experiment, the steady-state junctional conductance was normalized to the instantaneous value obtained at each potential and the data was pooled according to developmental age. The mean steady-state junctional conductance-voltage relationship for each age group was fit using a two-state Boltzmann distribution described previously for other voltage-dependent gap junctions. From this model, it was revealed that half-inactivation voltage for the transjunctional voltage-sensitive conductance shifted towards larger potentials by 10 mV, the equivalent gating charge increased by approximately 1 electron, and the minimal voltage-insensitive conductance exactly doubled (increased from 18 to 36%) between 4 and 18 days of development. Decay time constants were similar at all ages examined as rate increased with increasing transjunctional potential. This data provides the first direct experimental evidence for developmental changes in the regulation of intercellular communication within a given tissue. This information is consistent with the hypothesis that developmental expression of multiple gap junction proteins (connexins) may confer different regulatory mechanisms on intercellular communication pathways within a given cell or tissue.

Key Words gap junction · chick embryo · heart · intercellular communication · transjunctional voltage

Introduction

Gap junctions are specialized regions of the plasma membrane which permit the exchange of cytosolic ions and small molecules between adjacent cells in nearly all developing and fully differentiated tissues. These cell-to-cell channels appear as early as the 8-cell stage in developing mouse embryos (Lo & Gilula, 1979) and are well established in the precontractile chick heart, as evidenced by the presence of synchronous electrical activity in the 9-somite chick embryo (Fujii, Hirota & Kamino, 1981). Besides the obvious role of electrical coupling associated with normal cardiac function, gap junction channels are of sufficient size (10–20 Å in diameter) to permit the intercellular diffusion of small molecules of up to 1000 daltons in size between mammalian cells (Schwartzmann et al., 1981; Imanaga, Kameyama & Irisawa, 1987). Such molecules could include second messengers, which may play a role in coordinating cellular signals involved in a variety of functions (Gilula, Reeves & Steinbach, 1972; Lawrence, Beers & Gilula, 1978). Indeed, gap junctions have already been implicated in the passage of intracellular calcium acting as a second messenger for light emission in *Obelia* (Dunlap, Takeda & Brehm, 1987) and restoration of low-density lipoprotein receptor function by transfer of a UDP-galactose/UDP-N-acetylgalactosamine 4-epimerase product from normal to mutant cells lacking this enzyme (Hobbie et al., 1987). Because gap junctions appear so early in embryogenesis, they are often viewed as playing a fundamental role in growth control, pattern formation, and differentiation (Wolpert, 1978; Loewenstein, 1979; Mehta, Bertram & Loewenstein, 1986). The strongest evidence in support of this hypothesis is the demonstration that blockade of junctional communication by injection of gap junction antibodies or antisense RNA into developing embryos leads to decompaction of 4- to 8-cell embryos or tissue patterning defects in the area of the injected cells (Warner, Guthrie & Gilula, 1984; Fraser et al., 1987; Lee, Gilula & Warner, 1987; Bevilacqua, Loch-Caruso & Erickson, 1989). The contention that gap junctions play a direct role in the cell-to-cell transfer of developmental signals has been the subject of four recent reviews (Caveney, 1985; Green, 1988; Warner, 1988; Guthrie & Gilula, 1989) which all reveal that, although there is a large body of evidence to support this claim, the precise molecular mechanisms involved remain poorly understood.

Whatever the function, one of the key factors in the process of controlling the intercellular movement of a cytosolic signal-carrying molecule is the regulation of gap junction permeability. Several factors have been reported to affect short-term or long-term regulation of gap junction communication including intracellular pH, intracellular calcium, and a variety of protein kinases (Spray & Bennett, 1985; Loewenstein, 1987). One regulatory mechanism often found to regulate gap junctional communication in developing tissues (e.g., blastomeres), but less so in fully differentiated tissues (e.g., mammalian heart), is transjunctional voltage (V_j; Spray & Bennett, 1985). Recent observations in embryonic and neonatal ventricular myocyte pairs have successfully disputed the previously held contention that cardiac gap junctions are not regulated by transjunctional potentials (Rook, Jongsma & Van Ginneken, 1988; DeHaan, Chen & Penrod, 1989; DeHaan & Chen, 1990; Veenstra, 1990*a*,*b*). The apparent lack of V_j dependence in large conductance gap junctions, typical of adult mammalian ventricular myocytes, has been postulated to be the result of an increasing access resistance that develops as the number of channels within the gap junction plaque increases (Jongsma et al., 1990). In 7-day embryonic chick heart, it has been demonstrated that G_j is sensitive to transjunctional potentials above ±30 mV (DeHaan et al., 1989; DeHaan & Chen, 1990; Veenstra, 1990*a*,*b*). It was the purpose of this study to determine if any gradual changes in V_j-dependent regulation of cardiac gap junctions occur during embryonic chick heart development. Observations in paired 4-, 14-, and 18-day embryonic chick ventricular myocytes revealed a gradual loss of V_j sensitivity that coincides with increasing embryonic age and provides the first direct evidence for developmental regulation of intercellular communication within a given cell or tissue. A previously described Boltzmann model (Harris, Spray & Bennett, 1981; Spray, Harris & Bennett, 1981), which adequately describes the steady-state junctional conductance-voltage (G_j-V_j) relationship of numerous V_j-dependent gap junctions, was used to quantitatively assess the developmental changes in the half-inactivation voltage and slope of the G_j-V_j curve. Preliminary observations of these results have been presented elsewhere (Veenstra, 1990*b*,*c*).

Materials and Methods

Tissue Culture

Fertilized eggs from white Leghorn chickens were incubated at 37°C for 4-, 14-, or 18-days. The embryos were then decapitated, and the apical portions of the cardiac ventricles were dissected out and dissociated into their cellular components by the multiple cycle enzymatic dissociation procedure as previously described (DeHaan, 1970; Veenstra & DeHaan, 1986*a*). This procedure yielded a cell suspension containing 85–90% single cells plus several small clusters of two or more cells. An inoculum of 2×10^5 cells was added to plastic Petri dishes (Falcon Plastics, type 1008) treated with concentrated sulfuric acid (25 M) to permit cell attachment without extensive spreading (Veenstra & DeHaan, 1988). The plates were incubated in a humidified atmosphere of 95% air-5% CO_2 at 37°C for 22–28 hr (pH = 7.1). All cell pairs used for experimentation were termed 4-, 14-, or 18-day with reference to the age of the donor embryo.

Solutions

The dissociation medium, DM8, was composed of the following: 50 μg/ml crystalline trypsin (Worthington Enzymes, Freehold, NJ); 5.5 μg/ml deoxyribonuclease (Worthington, 9×10^{-4} U/mg); 1 mg/ml bovine serum albumin (fraction V fatty acid poor, Sigma Chemical, St. Louis, MO); NaCl, 116 mM; KCl, 5.4 mM; NaH_2PO_4, 1.0 mM; and dextrose, 5.5 mM. A similar solution was prepared for dissociating the 14- and 18-day tissue, but with 2 mg/ml collagenase (type 2, Worthington; 244 U/mg) in place in trypsin. Collagenase produces a higher yield of viable cells than trypsin from 14- or 18-day ventricle, owing to the larger content of connective tissue at these latter stages of development (Veenstra & DeHaan, 1986*a*). The culture medium, 21212, contained (by volume) 25% M199, 2% heat-inactivated horse serum, 67.5% K^+-free Ham's F12 (all from GIBCO, Grand Island, NY), 4% heat-inactivated fetal calf serum (Flow Laboratories, Horsham, PA), 1% L-glutamine, 0.5% penicillin-G (Sigma), and 1.3 mM KCl. During patch-clamp experiments, the cells are bathed in a protein-free balanced salt solution bath, BSS, composed of (in mM): NaCl, 142; KCl, 1.3; $MgSO_4$, 0.8; NaH_2PO_4, 0.9; $CaCl_2$, 1.8; dextrose, 5.5; and N-2-hydroxyethylpiperazine-N′-2-ethanesulfonic acid (HEPES, Sigma), 10. The pH was titrated to 7.2 by the addition of 1 N NaOH. Internal pipette solution, IPS, contained the following (in mM): K-glutamate, 120; NaCl, 15; KH_2PO_4, 1.0; $MgCl_2$-$6H_2O$, 4; glycoletherdiaminetetraacetic acid (EGTA, Sigma), 0.1; HEPES, 10; Na_2-ATP (Sigma), 3; and Na_2-phosphocreatine (CrP, Sigma), 3. The IPS was titrated to pH 7.1 with 1 N KOH. The ATP and CrP were added to the stock solution daily to improve the metabolic state of the cells during whole-cell recording. The EGTA was added to reduce trace amounts of Ca^{2+} in the IPS to $<10^{-7}$ M, but is not sufficient to act as a strong intracellular buffer.

Junctional Current and Conductance Measurements

Plates of cultured myocytes were rinsed 5–7 times with BSS and placed on the stage of an inverted phase contrast light microscope (Olympus IMT-2) for observation. All experiments were performed on paired myocytes at room temperature (20–22°C) according to standard double whole-cell patch-clamp procedures (Veenstra & DeHaan, 1986*b*, 1988). Patch electrodes, having tip resistances of 4–6 MΩ when filled with the IPS described above, were selected and coated with Sylgard (Dow Corning, Midland, MI) to reduce electrode capacitance prior to use. GΩ-seals and electrode capacitance compensation were achieved on both cells with a pair of patch-clamp amplifiers (BioLogic Model RK-300,

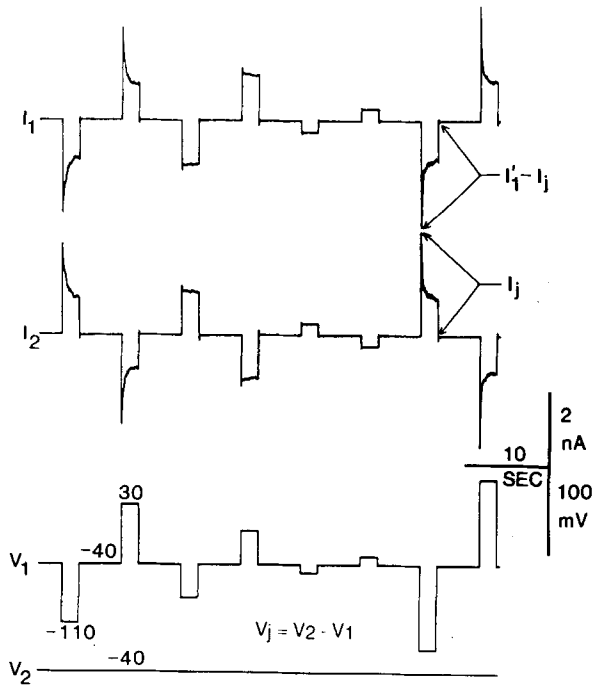

Fig. 1. Measurement of macroscopic junctional current (I_j). I_1 and I_2 are whole cell currents recorded under voltage-clamp conditions from each cell of an embryonic chick cell pair. V_1 and V_2 are the membrane voltages applied to each cell by separate patch-clamp amplifiers. Transjunctional voltage (V_j) is varied between ±100 mV by stepping V_1 from a holding potential of −40 mV to values ranging from −140 to +60 mV in 10-mV increments. Each voltage pulse is 2 sec in duration with a 5-sec recovery interval between pulses. V_2 is held constant at −40 mV, so $V_j = V_2 - V_1$. Junctional current (I_j) is observed in both current records as signals of opposite polarity, although there is also a small nonjunctional membrane current (I_1') associated with the V_1 voltage step. Hence, I_j is taken as the current signal recorded in I_2 during the V_1 voltage pulse. Macroscopic junctional conductance (G_j) can be calculated by dividing I_j by V_j

Meylan, France). The current signals were viewed directly with a digital storage oscilloscope (Gould Model 1604). Permanent records of the current and voltage signals for each cell were stored on VCR tape using a 2/4 channel VCR-based digital tape recorder (Neuro-Corder Model DR-484 digitizer and Sansui SV-7700 VHS VCR, Neuro Data Inst., NY) at a digital sample rate of 22 kHz/channel. For data analysis, the data was played back in analog form through a four-pole Butterworth filter (Ithaco Model 4302, Ithaca, NY) at a low-pass filter bandwidth of 125 Hz prior to digital sampling at 500 Hz by an A/D board (Data Translation Model DT2801A) installed in an IBM PC/AT.

The membrane voltages of both cells (V_1 and V_2) were independently controlled by separate voltage-clamp circuits, which permits direct measurement of macroscopic junctional current (I_j). A brief example of the experimental procedure is displayed in Fig. 1. Initially, V_1 and V_2 were set equal to each other ($V_1 = V_2 = -40$ mV) for 5 sec in order to determine the membrane holding currents for each cell (I_1 and I_2). A transjunctional voltage gradient ($V_j = V_2 - V_1$) was periodically produced by hyperpolarizing or depolarizing V_1 for 2 sec while V_2 was held constant. During each pulse, whole-cell current was applied by each patch-clamp amplifier in order to maintain V_1 and V_2 at their respective values. Under these conditions, I_j must be recorded as a current of opposite polarity and equal magnitude by the two voltage-clamp circuits (Veenstra & DeHaan, 1986*b*, 1988). However, only the change in I_2 during the V_j pulse is taken as a direct measure of I_j, as indicated by the arrows in Fig. 1. The change in I_1 is equal to the negative of I_j (as recorded in the partner cell) plus an additional nonjunctional membrane current (I_1') associated with altering V_1 (*see* Fig. 1). This procedure is identical to previously published methods and are described in more detail elsewhere (Veenstra, 1990*a*). All I_j pulses presented throughout this manuscript meet the above criteria.

Whole cell capacitive currents in response to a 10-mV depolarizing step (holding potential = −80 mV) were simultaneously recorded using a 1 MHz A/D board (RC Electronics, Santa Barbara, CA). Electrode resistances following patch break were determined from the capacitive current transients of each cell as previously described (Veenstra & DeHaan, 1988). Electrode resistances ranged from 10 to 34 MΩ (mean ± SEM: 19.8 ± 0.8 MΩ, $n = 48$) in all cells examined and did not vary systematically with age of the preparation (ANOVA, $P > 0.05$). Cell input resistances, as determined from whole-cell membrane I-V relationships between membrane potentials of −80 and 0 mV (Veenstra & DeHaan, 1988; Veenstra, 1990*a*), ranged from a minimum of 0.8 GΩ in an 18-day cell to a maximum of 20.5 GΩ in a 4-day cell. In all cases, series resistance was <5% of the cell input resistance, thus limiting variations between cell membrane and electrode voltages to less than 5% of the applied potential. In 20 of 27 cell pairs examined (eight 4-day, six 14-day, and six 18-day pairs), G_j ranged from 1.0 to 5.4 nS (2.79 ± 0.33 nS, mean ± SEM). These conditions are consistent with previous publications from 7-day cell pairs where the electrode resistance typically averaged <5% of the junctional resistance (G_j = 0 to 5 nS; Veenstra & DeHaan, 1988; Veenstra, 1990*a*). Occasionally, G_j values as high as 35 nS have been observed in 7-day cells (Veenstra & DeHaan, 1988). Similar observations were obtained in the present study, where the remaining 14- and 18-day cell pairs had G_j values ranging from 9.8 to 31.3 nS (18.57 ± 3.12 nS).

Mathematical Modeling of Steady-State Junctional Conductance-Voltage Curves

For each polarity, the steady-state G_j-V_j curve was fit by a Boltzmann equation of the form

$$G_j = \{(G_{max} - G_{min})/1 + \exp[A(V_j - V_0)]\} + G_{min} \quad (1)$$

where G_{max} is the maximum conductance (=1, normalized to instantaneous G_j for each voltage), G_{min} is the minimum conductance attained during a given experiment, V_0 is the voltage where G_j lies halfway between G_{max} and G_{min}, and A is a parameter expressing the steepness of the curve (Harris et al., 1981; Spray et al., 1981). The constant A can be expressed as zq/kT, where z is the number of equivalent electron charges q that act as the voltage sensor in the membrane to effect the transition from the open to closed conductance states, and kT represent Boltzmann's constant and absolute temperature, respectively. The Boltzmann relation determines the ratio of open to closed channels at equilibrium in terms of the energy difference (which varies with V_j) between the two states (Spray et al., 1981; Hille, 1984). The best fit of each steady-state G_j-V_j curve was determined by a customized nonlinear curve-fitting program (courtesy of W.N. Goolsby, Emory University) which utilizes the least squares crite-

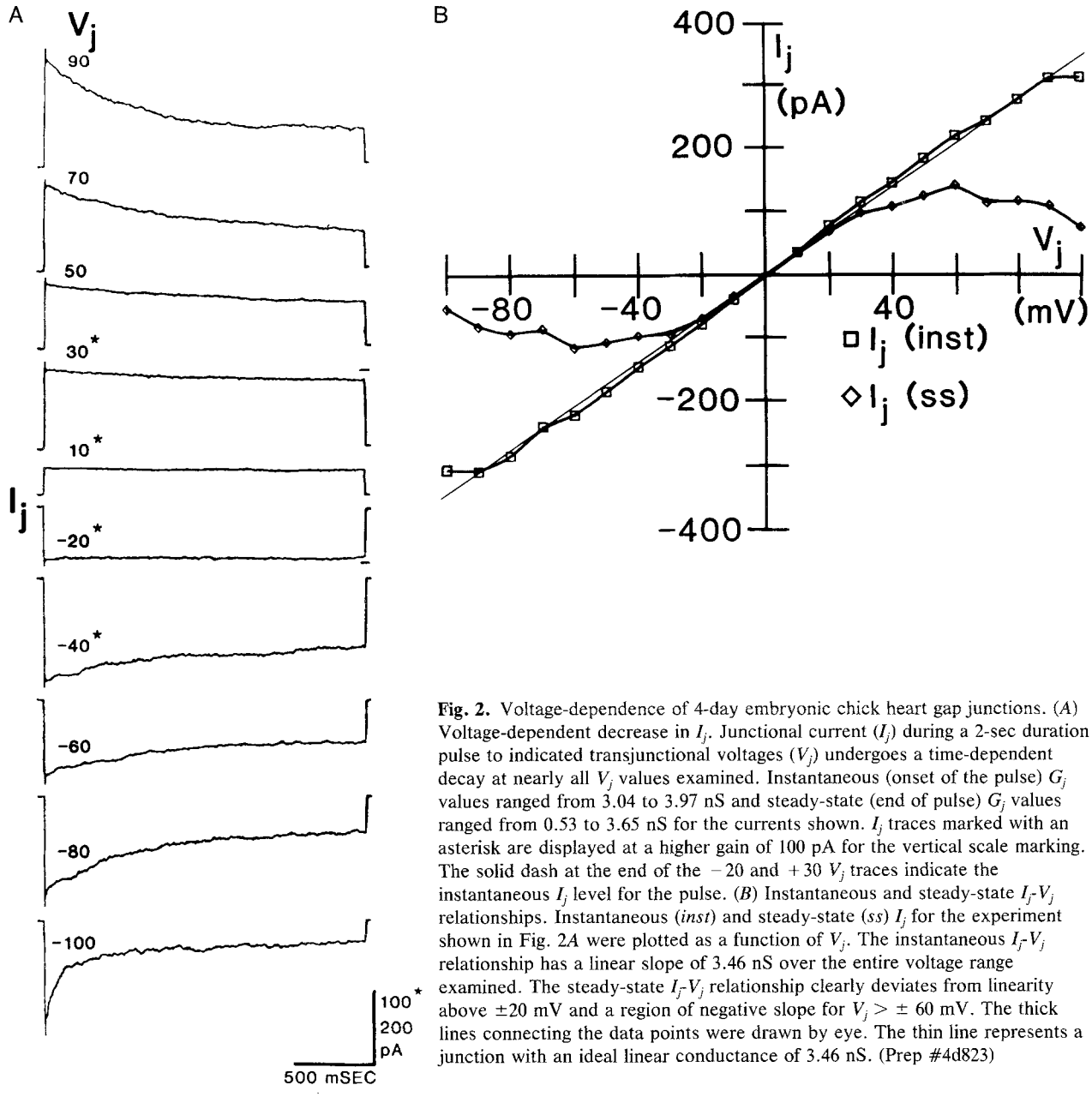

Fig. 2. Voltage-dependence of 4-day embryonic chick heart gap junctions. (*A*) Voltage-dependent decrease in I_j. Junctional current (I_j) during a 2-sec duration pulse to indicated transjunctional voltages (V_j) undergoes a time-dependent decay at nearly all V_j values examined. Instantaneous (onset of the pulse) G_j values ranged from 3.04 to 3.97 nS and steady-state (end of pulse) G_j values ranged from 0.53 to 3.65 nS for the currents shown. I_j traces marked with an asterisk are displayed at a higher gain of 100 pA for the vertical scale marking. The solid dash at the end of the −20 and +30 V_j traces indicate the instantaneous I_j level for the pulse. (*B*) Instantaneous and steady-state I_j-V_j relationships. Instantaneous (*inst*) and steady-state (*ss*) I_j for the experiment shown in Fig. 2*A* were plotted as a function of V_j. The instantaneous I_j-V_j relationship has a linear slope of 3.46 nS over the entire voltage range examined. The steady-state I_j-V_j relationship clearly deviates from linearity above ±20 mV and a region of negative slope for $V_j > \pm$ 60 mV. The thick lines connecting the data points were drawn by eye. The thin line represents a junction with an ideal linear conductance of 3.46 nS. (Prep #4d823)

rion to determine convergence. G_{max} = 1 since steady-state G_j (G_{ss}) was normalized to the maximum value obtained during each V_j pulse and G_{min} = minimum normalized G_j obtained during each experiment.

Results

Regulation of Junctional Current by Transjunctional Potentials in Embryonic Chick Heart

When the entire voltage protocol described above was applied to a pair of 4-day embryonic chick cells, a family of junctional current traces like those shown in Fig. 2*A* were generated. The four traces marked with an asterisk are shown at twice the amplification of the rest of the currents for the purpose of visualizing any small time-dependent changes in I_j that occur at these potentials. A rapid rise in I_j was evident with the onset of every V_j pulse, which increases in direct proportion to the incremental increase in V_j. At V_j = 10 mV, there was no discernable change in the amplitude of I_j during the pulse shown here. However, this is not the case for the rest of the I_j pulses in this example. The solid lines at the end of the −20 and +30 mV V_j pulses, marking the initial I_j value measured during the first 10 msec of the pulse, indicate

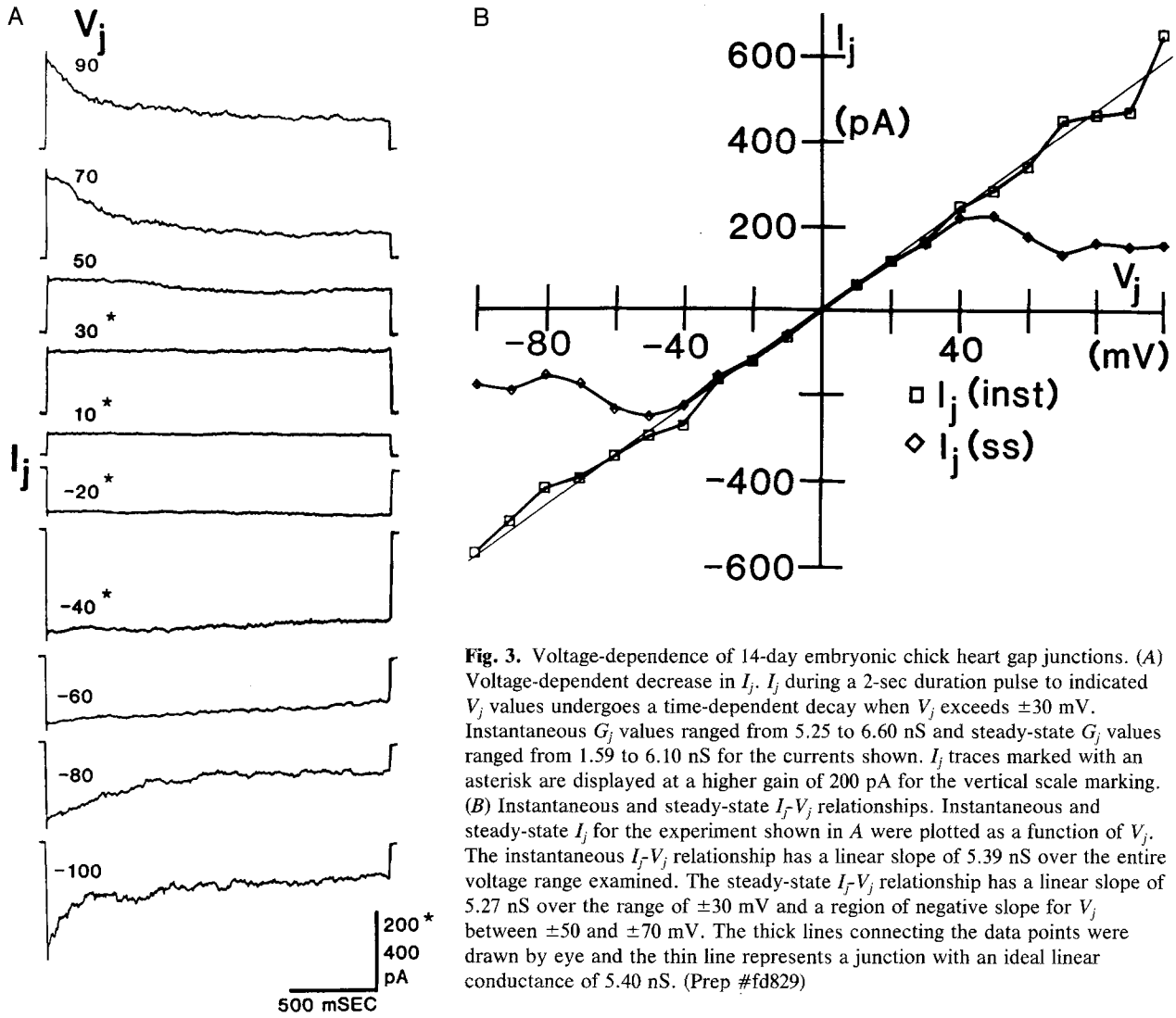

Fig. 3. Voltage-dependence of 14-day embryonic chick heart gap junctions. (*A*) Voltage-dependent decrease in I_j. I_j during a 2-sec duration pulse to indicated V_j values undergoes a time-dependent decay when V_j exceeds ±30 mV. Instantaneous G_j values ranged from 5.25 to 6.60 nS and steady-state G_j values ranged from 1.59 to 6.10 nS for the currents shown. I_j traces marked with an asterisk are displayed at a higher gain of 200 pA for the vertical scale marking. (*B*) Instantaneous and steady-state I_j-V_j relationships. Instantaneous and steady-state I_j for the experiment shown in *A* were plotted as a function of V_j. The instantaneous I_j-V_j relationship has a linear slope of 5.39 nS over the entire voltage range examined. The steady-state I_j-V_j relationship has a linear slope of 5.27 nS over the range of ±30 mV and a region of negative slope for V_j between ±50 and ±70 mV. The thick lines connecting the data points were drawn by eye and the thin line represents a junction with an ideal linear conductance of 5.40 nS. (Prep #fd829)

that I_j decreased slightly during each V_j pulse. This decrease in I_j became more prominent at larger V_j values.

The voltage-dependent decline of I_j was best illustrated by plotting the instantaneous and steady-state I_j values as a function of V_j, as shown in Fig. 2*B*. Instantaneous I_j was determined by taking the average current during the first 10 msec of each pulse and plotting this value as a function of V_j. These results are illustrated by the open squares in Fig. 2*B*. The I_j-V_j relationship was linear with the slope of the line being equal to the junctional conductance (G_j) of the preparation (3.46 nS). A different relationship is found when steady-state I_j, measured during the last 10 msec of the V_j pulse, is plotted accordingly. These results are illustrated by the open diamonds in Fig. 2*B*. Steady-state I_j was virtually identical to the instantaneous current at ±10 mV, but the steady-state I_j-V_j relationship deviates further from linearity as V_j increases in either direction. Beyond ±60 mV, steady-state I_j actually decreases with increasing V_j, producing a negative slope conductance for the junctional membrane (for a definition, *see* Jack, Noble & Tsien, 1983) in the ±60 to ±100 mV range of potentials. This example was characteristic in all 4-day cell pairs (n = 8) examined. The slope of the instantaneous I_j-V_j relationships ranged from 1.0 to 3.85 nS for the eight 4-day cell pairs (2.19 ± 0.48 nS, mean ± SEM).

Slightly different results were obtained when 14-day cell pairs were examined using the same procedures described above. In Fig. 3*A*, the four I_j traces marked with an asterisk are again displayed with twice the amplification of the other I_j traces. In these records, a time-dependent decrease in I_j was not evident until $V_j \geq \pm 40$ mV. This observation was further substantiated by comparing the instantaneous and steady-state I_j-V_j relationships for this

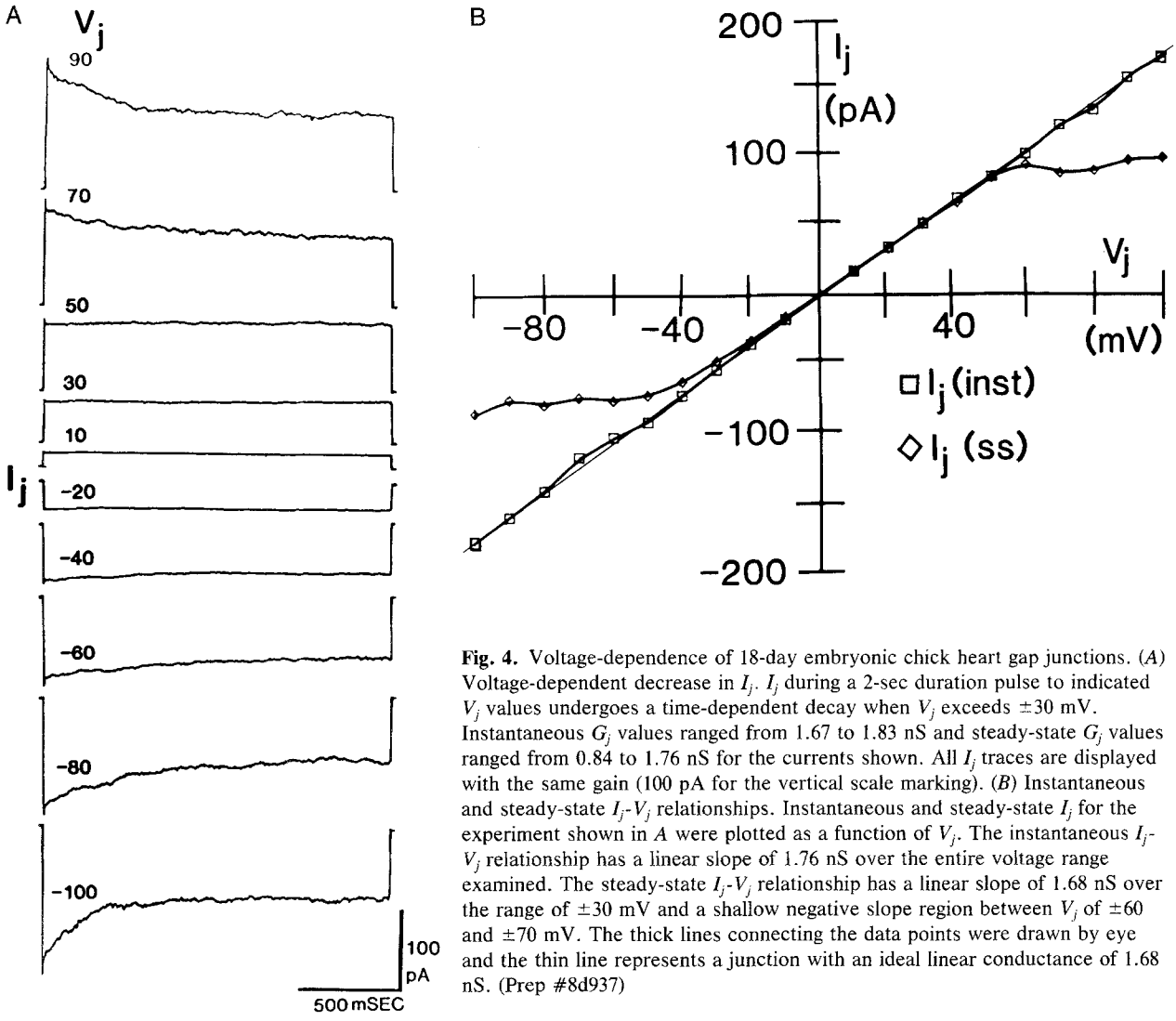

Fig. 4. Voltage-dependence of 18-day embryonic chick heart gap junctions. (*A*) Voltage-dependent decrease in I_j. I_j during a 2-sec duration pulse to indicated V_j values undergoes a time-dependent decay when V_j exceeds ±30 mV. Instantaneous G_j values ranged from 1.67 to 1.83 nS and steady-state G_j values ranged from 0.84 to 1.76 nS for the currents shown. All I_j traces are displayed with the same gain (100 pA for the vertical scale marking). (*B*) Instantaneous and steady-state I_j-V_j relationships. Instantaneous and steady-state I_j for the experiment shown in *A* were plotted as a function of V_j. The instantaneous I_j-V_j relationship has a linear slope of 1.76 nS over the entire voltage range examined. The steady-state I_j-V_j relationship has a linear slope of 1.68 nS over the range of ±30 mV and a shallow negative slope region between V_j of ±60 and ±70 mV. The thick lines connecting the data points were drawn by eye and the thin line represents a junction with an ideal linear conductance of 1.68 nS. (Prep #8d937)

14-day cell pair (Fig. 3*B*). The instantaneous (open squares) and steady-state (open diamonds) I_j values for $\pm 10 \leq V_j \leq \pm 30$ mV were virtually identical with linear slopes of 5.39 and 5.27 nS, respectively. Once again, the instantaneous I_j-V_j relationship is essentially linear over the entire V_j range examined. However, the steady-state I_j relationship does deviate from linearity once V_j exceeds ±30 mV. Steady-state I_j is observed to decrease with increasing V_j, thereby producing a region of negative slope conductance for the junctional membrane, which is restricted to a region between ±50 and ±70 mV. Steady-state I_j remained relatively constant beyond V_j of ±80 mV. Similar results were obtained from all eight 14-day cell pairs examined. The slope of the instantaneous I_j-V_j relationships ranged from 0.95 to 17.80 nS for the eight 14-day cell pairs (6.59 ± 2.19 nS). Only two of eight 14-day cell pairs had an instantaneous $G_j > 5.40$ nS.

At 18-days of embryonic development, the transjunctional voltage-dependence of cardiac gap junctions was even less apparent, relative to 4- and 14-day embryonic chick heart. The family of junctional current traces presented in Fig. 4*A* was obtained from an 18-day cell pair under identical experimental conditions to the above studies and again reveals a lack of V_j-dependent decline in I_j below ±30 mV. However, even though a time- and V_j-dependent decline in I_j was clearly evident at larger potentials ($V_j > \pm 50$ mV), a substantial fraction of I_j remained at the end of the −100 mV pulse. The instantaneous I_j-V_j relationship (open squares, Fig. 4*B*) for 18-day heart was once again linear throughout the entire V_j range examined (slope = 1.76 nS for this preparation). The steady-state I_j-V_j relationship (open diamonds, Fig. 4*B*) was once again nonlinear, but lacks the regions of negative slope conductance previously observed in the 4- and 14-day

preparations. Similar results were obtained from all eleven 18-day cell pairs examined. The slope of the instantaneous I_j-V_j relationships ranged from 1.77 to 31.30 nS for the eleven 18-day cell pairs (10.47 ± 3.23 nS).

The time course of the decline in I_j was also examined at each V_j between ±50 to ±100 mV by fitting exponential functions to the decay phase of I_j. Examples of the best fits obtained for a 4-day cell pair experiment are illustrated in Fig. 5. The corresponding V_j is indicated to the left of each trace, and the smooth line represents the best fit of the data obtained using monoexponential or biexponential functions. The arrows along the right margin indicate the steady-state current predicted by the idealized fit of the data. There is close agreement between the experimental data and the theoretical curves regarding the decay time course and steady-state I_j values with few exceptions. All of the traces in Fig. 5 were fit with monoexponential functions except that of −100 mV, which is well defined by a biexponential function having time constants of 65 and 905 msec. In contrast, the +100 mV trace from this same cell pair could be fit only by a monoexponential function. Overall, 75% of all I_j traces obtained from eight 4-day cell pairs were best fit by single exponential functions. Biexponential fits most commonly occurred at the larger voltages of low G_j pairs and produced time constants of less than 100 msec for the first exponential and 250 to 1500 msec for the second exponential component.

Figure 5 also provides another observation about whether I_j actually achieves a steady-state during the 2 sec duration of each pulse. For the example shown in Fig. 5, steady-state I_j during the +50 mV pulse was 125 pA while the exponential fit predicted a steady-state I_j of 104 pA (17% less than the level achieved during the pulse). This corresponds to a normalized G_{ss} of 0.64 and 0.53 for the experimental and theoretical conditions, respectively. At all other V_j values, the difference between experimental and predicted steady-state values was 7% (at +60 mV) or less. Similar discrepancies arose in only two of eight 4-day cell pairs at select V_j values where the time constants exceeded 1 sec. These results indicate that I_j decays to within 5% of predicted steady-state values at the end of each 2-sec pulse.

These procedures were also applied to all 14- and 18-day cell pairs examined, this time yielding single exponential functions in over 90% of all trials. The monoexponential time constants for all ages are summarized in Table 1. These results reveal that, in spite of the increasing linearity of the steady-state I_j-V_j relationships at low voltages and the observed rise in residual steady-state I_j with developmental age, any observed differences in the time constants between age groups were not significant (nonparametric analysis of variance, $P > 0.05$). Time constants were observed to decrease as V_j increased in either direction, consistent with previous observations for other V_j-dependent gap junctions (Harris et al., 1981).

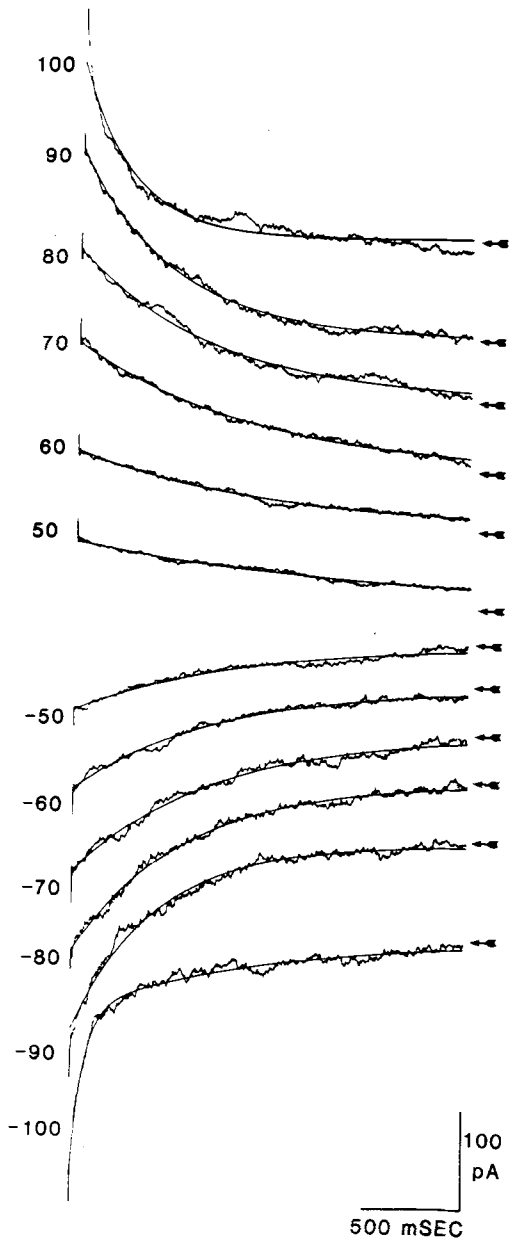

Fig. 5. Decay time constants of junctional current (I_j). The smooth line depicts the best fit of the decay phase of each I_j trace recorded at the indicated V_j (left margin). The arrow along each right margin indicates the predicted steady-state current for each trace. Time constants for the traces are (in msec): +100, 260; +90, 456; +80, 692; +70, 881; +60, 1010; +50, 1590; −50, 783; −60, 685; −70, 697; −80, 565, −90, 425; −100, 65 and 902. (Prep #4d823)

Table 1. Decay time constants of junctional current

V_j (mV)	4-Day (msec) (mean ± SEM, N)	14-Day (msec) (mean ± SEM, N)	18-Day (msec) (mean ± SEM, N)
−100	−196 ± 83 (7)	−184 ± 29 (8)	−168 ± 34 (11)
−90	−330 ± 102 (7)	−188 ± 30 (8)	−205 ± 45 (11)
−80	−330 ± 94 (7)	−290 ± 61 (8)	−313 ± 85 (8)
−70	−310 ± 102 (7)	−427 ± 68 (8)	−280 ± 62 (11)
−60	−390 ± 102 (7)	−592 ± 220 (8)	−378 ± 65 (11)
−50	−430 ± 90 (6)	−484 ± 115 (6)	−632 ± 102 (11)
50	−650 ± 129 (7)	−557 ± 188 (8)	−631 ± 230 (9)
60	−510 ± 106 (7)	−496 ± 163 (8)	−459 ± 140 (11)
70	−390 ± 91 (7)	−436 ± 99 (8)	−378 ± 99 (11)
80	−320 ± 102 (7)	−274 ± 65 (8)	−277 ± 70 (11)
90	−235 ± 53 (7)	−179 ± 39 (7)	−224 ± 42 (11)
100	−210 ± 49 (7)	−205 ± 47 (5)	−234 ± 54 (11)

Table 2. Developmental differences in V_j-dependent cardiac gap junctions

Age (days)	Experimental values			Theoretical parameters[a]		
	N	G_{max}	G_{min}	A	V_0 (mV)	z
4	8	1.0	0.18	0.058	42	1.47
7	4	1.0	0.28	0.068	45	1.72
14	8	1.0	0.28	0.096	50	2.44
18	11	1.0	0.36	0.100	52	2.54

[a] Theoretical parameters are determined from the Boltzmann equation described in Materials and Methods.
[b] All 7-day values were obtained from Veenstra (1990*a*).

Steady-State Junctional Conductance-Voltage Relationships of Developing Chick Heart

Because instantaneous I_j (or G_j) and V_j were linearly related, steady-state G_j (G_{ss}) could be normalized to the instantaneous G_j (G_{inst}) of each pulse. The normalized data for each experiment was then fit with Eq. (1). Figure 6 displays the mean steady-state junctional conductance-voltage relationship and the calculated best fit G_{ss}/G_{inst} *vs.* V_j) for each developmental age. The normalized G_{ss}-V_j curve for 4-day chick heart is illustrated in Fig. 6*A*, where the open squares and error bars represent the mean (±SEM) of normalized G_{ss} at each V_j for all eight experiments. G_j declined gradually to a minimum of 0.18 at ±100 mV, with the slope of the curve being steepest between ±10 and ±50 mV. The normalized G_{ss}-V_j relationship compiled from all eight 14-day chick heart experiments (Fig. 6*B*), was also symmetrical around 0 mV and leveled off to a minimum value (28% of maximum) at ±100 mV. However, the reduction in G_j within the ±0 to ±30 mV range was approximately 1/3 of that observed in 4-day heart. Also, the largest decrease in G_j of 14-day heart occurred between the V_j values of ±40 to ±70 mV, which is shifted outward by approximately 30 mV relative to 4-day heart. The normalized G_{ss}-V_j relationship for all eleven 18-day chick heart experiments is presented in Fig. 6*C*. When compared to Fig. 6*A* and *B*, some differences are apparent. In 18-day heart, G_j remained even closer to the maximum conductance (= 1) within the ±0 to ±30 mV range, with the largest decrease in G_j occurring between the V_j values of ±40 to ±70 mV. Although G_j is shifted towards still higher values in this range of V_j, the shape of the curve closely resembles that of the 14-day chick heart. Second, the minimum conductance was 36% of maximum, which produces the observed differences between G_{ss} of 14- and 18-day heart at some of the higher V_j values. Comparison of the 4- and 18-day normalized G_{ss}-V_j relationships clearly indicates that developmental changes in G_j regulation have occurred over this two week period, with G_j being relatively higher in 18-day heart than 4-day heart at all V_j values examined. This result was confirmed by determining the area under the curve for each experiment and subjecting these values to ANOVA analysis. Only the 4- and 18-day curves were found to be significantly different ($P < 0.001$).

The solid line for each graph in Fig. 6 represents the theoretical fit of the data using the Boltzmann equation as described in Materials and Methods (Spray et al., 1981; Veenstra, 1990*a*). This mathematical model provides a good fit of the normalized G_{ss}-V_j relationships for all three embryonic ages. A summary of the relevant experimental and theoretical parameters are presented in Table 2. Initial comparisons of these parameters reveal a gradual increase in the voltage-insensitive component of G_j (G_{min}), an outward shift in the half-inactivation voltage for the voltage-sensitive component of $G_j(V_0)$, and an increase in the equivalent valence (z) of the voltage-sensing portion of the gap junction channel. All of these changes are consistent with a gradual loss of V_j sensitivity (and increasing energy requirement for the conformational transition from the open to closed state) that occurs with increasing developmental age. ANOVA analysis of the changes in G_{min}, V_0, and slope factor A (as determined for each individual experiment) between these three age groups revealed that only the differences in G_{min} between 4- and 18-day heart were significant ($P < 0.001$). As evident in Table 2, the parameters describing the 7-day heart normalized G_{ss}-V_j curve are intermediate to those of 4- and 14-day chick heart. ANOVA analysis of the area, G_{min}, V_0, and slope factor A for all four ages examined to date again indicated that the

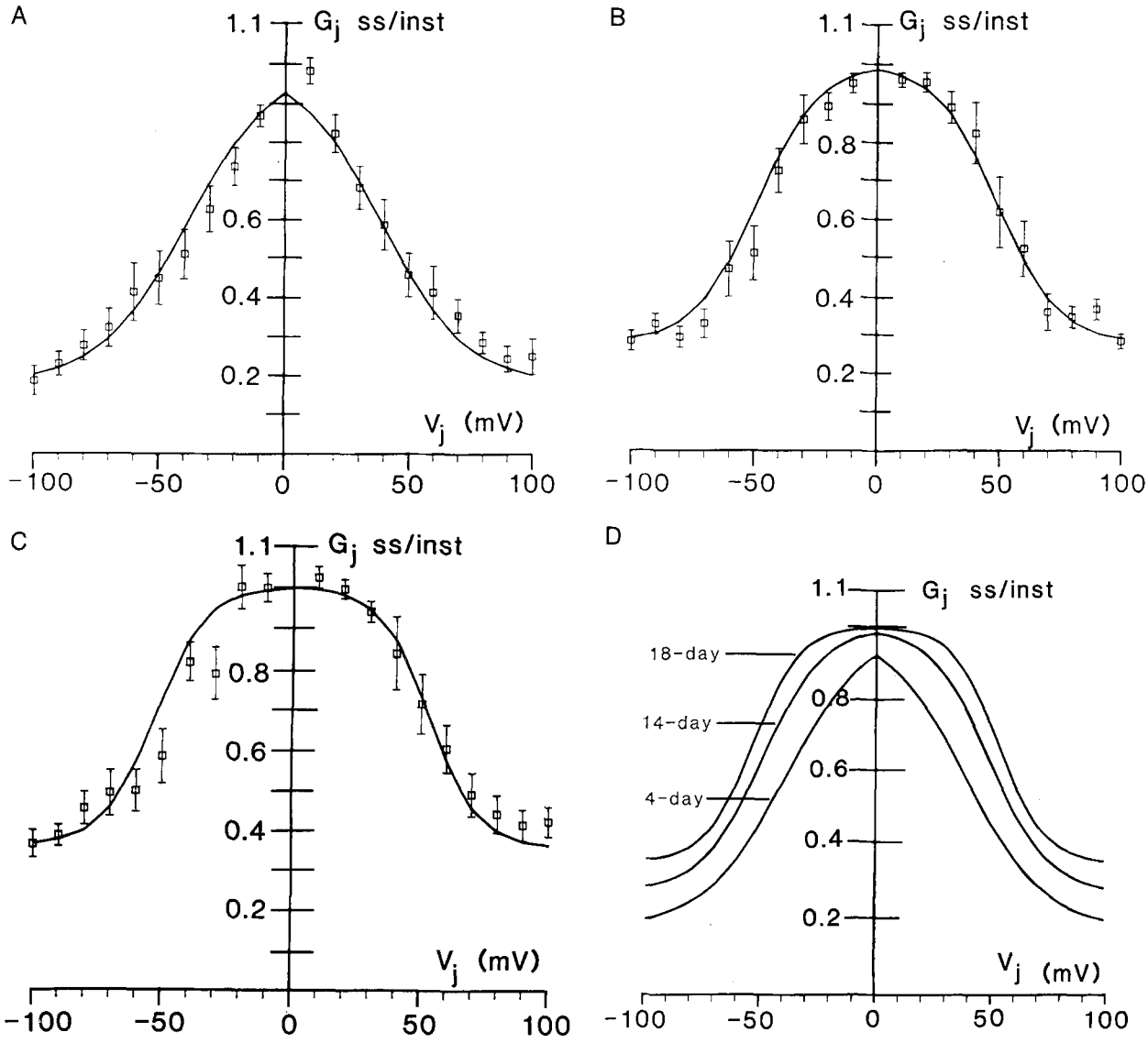

Fig. 6. Voltage-dependent decline in steady-state G_j. Steady-state G_j was normalized to instantaneous G_j at each V_j for every experiment and the data pooled according to developmental age of the preparation. Each point represents the mean ± SEM for each sample population. The solid line is a theoretical fit of the data assuming a two-state Boltzmann distribution described in the text. (*A*) Steady-state G_j-V_j relationship for 4-day chick ventricular cell pairs. Steady-state G_j was reduced by 41–49% at ±40 mV and attained a minimum value of 0.19 at V_j = ±100 mV. n = 8 experiments. (*B*) Steady-state G_j-V_j relationship for 14-day chick ventricular cell pairs. Steady-state G_j was reduced by only 18–27% at ±40 mV and attained a minimum value of 0.29 at V_j = ±100 mV. n = 8 experiments. (*C*) Steady-state G_j-V_j relationship for 18-day chick ventricular cell pairs. Steady-state G_j was reduced by only 1% at ±20 mV (16–18% at ±40 mV) and attained a minimum value of 0.36 at ±100 mV. n = 11 experiments. (*D*) Superimposed Boltzmann curves for all three developmental ages as presented in the previous panels illustrating the relative changes in the steady-state G_j-V_j relationship that are evident during development

area and G_{min} for the 4- and 18-day heart G_{ss}-V_j relationships were significantly different ($P < 0.001$).

Behavior of Gap Junction Channels

The results in this study indicate that the macroscopic (total) junctional currents and conductances decrease by a first-order process that depends on V_j and developmental age. Presumably, these records are the result of the summed activity of all of the individual channels in the gap junction. This can be mathematically represented by the equation

$$G_j = (\gamma j \cdot N \cdot P_o)_1 + (\gamma j \cdot N \cdot P_o)_2 + \ldots + (\gamma j \cdot N \cdot P_o)_n, \quad (2)$$

where γj = single channel conductance, N = number of channels, P_o = fraction of open channels (open-state probability), assuming that there are n distinct populations of gap junction channels in a cell pair (Veenstra & DeHaan, 1989). As stated previously, gap junction channel activity can be observed under the appropriate experimental conditions, namely high junctional and nonjunctional resistances (Veenstra & DeHaan, 1986*b*, 1988). In 7-day embryonic chick heart, at least two conductance states (60 and 160 pS, Veenstra & DeHaan, 1986*b*, 1988; Veenstra, 1990*a*; or 40, 80, 160, and 240 pS, Chen & DeHaan, 1989) have been reported. The 160-pS channel is the one most frequently observed in cell pairs at room temperature, provided $G_j < 2$ nS. For the large 160-pS channel in 7-day embryonic chick heart, it was revealed that the single gap junction channel currents are linearly related to V_j (Veenstra & DeHaan, 1988; Veenstra, 1990*a*). This channel was also observed to undergo a reduction in open-state probability when repeatedly stepped to V_j = 80 mV (Veenstra, 1990*a*). Similar behavior has been observed on occasion in 4-, 14-, and 18-day cell pairs. One such example is shown in Fig. 7, where a train of five 80-mV V_j pulses was applied to a 14-day cell pair. Upward deflections in I_j reflect the opening of gap junction channels, as indicated by the arrow in the fourth panel from the top in Fig. 7. At least one channel (γj = 170 pS) was observed to close during every pulse. When one averages the current of all five traces with respect to time (ensemble averaging, bottom panel, Fig. 7), one obtains a trace that is well fit by a monoexponential function (solid line) with a time constant of 55 msec. This data suggests that the exponential decay of I_j observed in high G_j gap junctions results from the V_j-dependent reduction in open-state probability (P_o) for a population of 160-pS gap junction channels. It remains to be determined if any of the other gap junction channel conductances also exhibit voltage-dependent gating.

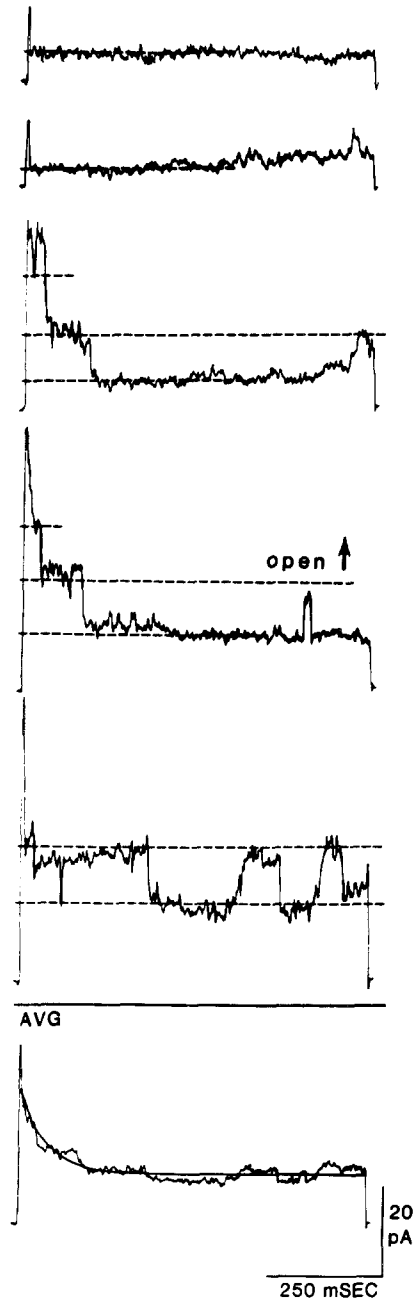

Fig. 7. V_j-dependent closure of individual gap junction channels. A train of 80 mV, 750 msec duration V_j pulses was applied in 10 sec intervals to a 14-day cell pair with $G_j < 1$ nS. All five individual traces reveal the closure of one or more channels (dashed lines indicate discrete 170 pS levels) during the V_j pulse. Bottom trace (*AVG*) is the ensemble average of junctional current compiled from all five traces with 2 msec time resolution. The decay phase of the average current follows a monoexponential time course, as indicated by the solid line, with a time constant of 55 msec. Analog filter frequency = 200 Hz and digital sample rate = 500 Hz. (Prep #fd804)

Discussion

In this study, the V_j-dependence of embryonic chick heart gap junctions was quantitatively assessed at 4-, 14-, and 18-days of development. The results demonstrate that a gradual loss in V_j-dependent regulation of G_j occurs with increasing embryonic age, as evidenced by the 10-mV outward shift in the half-inactivation voltage (V_0) and the twofold increase in the V_j-insensitive G_j component (G_{min}) between 4 and 18 days of embryonic development. The slope of the steady-state G_j-V_j curve also increased by 50%, which calculates to an equivalent increase in the gating charge of one electron. These changes were also observed as a progressive increase in the linearity of the steady-state I_j-V_j relationships at low voltages and a reduction in the negative slope region

of the steady-state I_j-V_j relationships for the three different ages examined.

V_j-dependent behavior has been observed to gradually diminish as G_j increases, presumably due to an increase in the cytoplasmic access resistance relative to the junctional resistance of the preparation (Rook et al., 1988; Jongsma et al., 1990). In the present investigation, eight 4-day, six 14-day, and six 18-day cell pairs all had similar G_j values of 1–5 nS. Yet the developmental changes in V_j sensitivity were still evident in these pairs, as demonstrated in Figs. 2–4. Furthermore, even the lone 31-nS 18-day cell pair included in this investigation demonstrated marked V_j dependence consistent with the lower G_j 18-day cell pairs ($G_{ss} > 0.9$ at ± 40 mV, declining to 0.31 at ± 100 mV). Hence, the observed changes in V_j dependence of the embryonic chick cardiac gap junctions are not correlated with any systematic age-dependent increases in access resistance or G_j.

Other observations revealed strong similarities in cardiac gap junction behavior throughout embryonic development. First, the instantaneous I_j-V_j relationships were linear at all ages examined, which indicates that all gap junctions behave as simple ohmic resistors in the resting state. Second, the G_j decay time constants were similar at all ages examined, becoming faster as V_j increases. Both of these observations are a common feature of other V_j-dependent gap junctions. Although a rigorous examination of kinetic parameters has not been performed beyond curve fitting the decay phase of G_j, the obvious similarity in the time constants indicates that a common V_j-dependent gating mechanism may be involved at all ages of cardiac development. Third, V_j-dependent modulation of I_j is achieved at least in part by a decrease in the open-state probability of the 160-pS channel. This observation is in agreement with earlier work in 7-day heart (Veenstra, 1990*a*) and is also consistent with the hypothesis that one class of channels may be involved in gating at all embryonic ages. More information is required about the other conductances observed in embryonic chick heart gap junctions before any conclusions can be made regarding their V_j-dependent behavior. It is important to note that the Boltzmann equation (1) does not distinguish between prospective populations of channels having different V_j sensitivities. For instance, the V_j-insensitive component of the normalized G_{ss}-V_j curve (G_{min}) could result from incomplete closure of a single population of gap junction channels or from a second population of channels which is not gated by transjunctional potentials.

The gap junctions which show the strongest V_j dependence of steady-state G_j are those amphibian blastomeres ($V_0 = 15$ mV, $z = 6$, $G_{min} = 0.05$: Harris et al., 1981; Spray et al., 1981). Recently, a *Xenopus* embryonic gap junction protein has been cloned and sequenced (Ebihara et al., 1989). The sequence of this 38-kD protein is 30–40% homologous to the well-characterized gap junction proteins of rat liver and heart, respectively named rat connexin32 and connexin43 (Beyer, Paul & Goodenough, 1987). The predicted topology of connexin38, based on hydropathicity profiles, bears a strong resemblance to connexin32 and connexin43 with the exception of a fifth hydrophobic putative transmembrane segment near the COOH-terminus (Ebihara et al., 1989). Neither the unique fifth hydrophobic domain of Cx38 nor any of the four transmembrane domains common to all connexins resemble the highly charged S4 segment present in all voltage-sensitive ion channel proteins (Catterall, 1988). The involvement of this S4 α-helix of the rat sodium channel II in the voltage-dependent activation process has been confirmed by site-directed mutagenesis (Stühmer et al., 1989; Auld et al., 1990). However, embryonic gap junction channels are already open at rest, as evidenced by the linear instantaneous I_j-V_j relationships. Furthermore, the observation that the recovery time constant from inactivation is 5 to 7 times slower than the V_j-dependent decay time constant qualitatively resembles that of sodium channel inactivation (Veenstra, 1990*a*). Therefore, V_j-dependent gating of gap junctions may involve distinct cytoplasmic domains of the channel protein, as has been described for sodium channel inactivation (Stühmer et al., 1989; Vassilev, Scheuer & Catterall, 1989).

The precise molecular composition of embryonic chick heart gap junctions is not known. Recently, Musil, Beyer & Goodenough (1990) have cloned and sequenced an embryonic chick connexin43 from a whole 10-day chick embryo cDNA library, which is 92% homologous to rat connexin43 in primary amino acid composition. This member of the connexin family was demonstrated to be post-translationally phosphorylated and expressed in chick lens epithelial cells. Along with chick connexin43, two other clones were identified which hybridized at reduced stringency to the rat connexin43 probe. These two independent clones have also been sequenced and are found to code for two connexin-related proteins with predicted molecular masses of 42 and 45 kD and are referred to as chick connexin42 and chick connexin45, respectively (Beyer, 1990). Northern blots of embryonic chick heart reveal that all three chick connexins are expressed in 12-day embryonic heart. Further investigation revealed that all three chick connexin mRNAs are expressed in higher quantities in embryonic heart (peak at day 9) than in adult heart, but connexin45 and connexin42 show the largest decline in relative amount from embryonic to adult heart. Coexpression of related gap junction proteins, connexin32 and connexin26, has also been observed in rat liver (Zhang & Nichol-

son, 1989). This new information about connexin coexpression is consistent with the hypothesis that changes in V_j-dependent gating of embryonic chick heart gap junctions may result from developmental changes in relative amounts of distinct connexins which possess different V_j-dependent gating properties.

What physiological role V_j-dependent gap junctions play in the developing heart remains to be answered. Although the heart undergoes a 1000-fold increase in size during embryogenesis, the time required for spread of the wave of excitation remains relatively constant. This is due to an equal increase in conduction velocity which may partially reflect an increase in junctional conductance, although cellular geometry and action potential upstroke velocity are also important determinants of conduction velocity which change with development (DeHaan & Chen, 1990). The effects of V_j-dependent gating of gap junction channels with regard to the propagation of a cardiac action potential in well-coupled tissues are likely to be negligible, but this mechanism could serve a protective role as a rapid means for partially uncoupling healthy heart cells from damaged or compromised (ischemic) cells (Veenstra, 1990*a*). The influence of V_j-dependent gap junctions in poorly coupled and damaged cardiac tissues on conduction velocity remain to be determined.

Another possible role for V_j-dependent gap junctions is in the control of cellular growth or differentiation, which is proposed to be influenced by the concentration profiles of signal-carrying molecules that relay positional information about the cell's location within the tissue or embryo (Wolpert, 1978). The interaction of cells with their local environment can occur through both extracellular (extracellular space or cell-matrix) and intercellular (cell-cell) pathways. Such regional cues have been implicated in the regulation of beat rate in developing precardiac cells (Satin, Fujii & DeHaan, 1988), although the precise molecular nature of the inductive signal remains unknown. The patterning of a diffusable cytosolic morphogen will depend on the junctional permeability within and between tissues. If the signal-carrying molecule possesses a net electrical charge (or is an ion, e.g. Ca^{2+}), then its distribution can be influenced by cytoplasmic voltage gradients (Cooper, Miller & Fraser, 1989). Such weak electric fields are commonly found in developing and regenerating tissues (Winkel & Nuccitelli, 1989). Another consequence of junctional communication is that it increases the sensitivity of the electrotonically coupled cells to weak electric fields, with the field effects being strongest at the boundaries (Cooper, 1984). It has been speculated that the regulation of junctional communication by transjunctional potentials confers plasticity of intercellular communication boundaries in developing tissues, which could influence the spread of developmental signals (Harris, Spray & Bennett, 1983). Although this concept remains to be proven, what is apparent is that there appears to be a pattern emerging, where the most V_j-sensitive gap junction channels are typically present during the earliest stages of development.

The author wishes to thank Drs. Alain Vinet and Richard Oates for helpful advice on statistical analysis, Dr. Hong-Zhan Wang and Mr. Mark Chilton for technical assistance, and Dr. Eric Beyer for helpful discussions. This study was supported by National Institutes of Health Grant #HL42220 and American Heart Association Grant-in-Aid #880708.

References

Auld, V.J., Goldin, A.L., Krafte, D.S., Catterall, W.A., Lester, H.A., Davidson, N., Dunn, R.J. 1990. A neutral amino acid change in segment IIS4 dramatically alters the gating properties of the voltage-dependent sodium channel. *Proc. Natl. Acad. Sci. USA* **87:**323–327

Bevilacqua, A., Loch-Caruso, R., Erickson, R.P. 1989. Abnormal development and dye coupling produced by antisense RNA to gap junction protein in mouse preimplantation embryos. *Proc. Natl. Acad. Sci. USA* **86:**5444–5448

Beyer, E.C., Paul, D.L., Goodenough, D.A. 1987. Connexin43: A protein from rat heart homologous to a gap junction protein from liver. *J. Cell Biol.* **105:**2621–2129

Beyer, E.C. 1990. Molecular cloning and developmental expression of two chick embryo gap junction proteins. *J. Biol. Chem.* **265:**14439–14443

Catterall, W.A. 1988. Structure and function of voltage-sensitive ion channels. *Science* **242:**50–61

Caveney, S. 1985. The role of gap junctions in development. *Annu. Rev. Physiol.* **47:**319–335

Chen, Y.-H., DeHaan, R.L. 1989. Cardiac gap junction channels shift to lower conductance states when temperature is reduced. *Biophys. J.* **55:**152*a*

Cooper, M.S. 1984. Gap junctions increase the sensitivity of tissue cells to exogenous electric fields. *J. Theor. Biol.* **111:**123–130

Cooper, M.S., Miller, J.P., Fraser, S.E. 1989. Electrophoretic repatterning of charged cytoplasmic molecules within tissues coupled by gap junctions by externally applied electric fields. *Dev. Biol.* **132:**179–188

DeHaan, R.L. 1970. The potassium-sensitivity of isolated embryonic heart cells increases with development. *Dev. Biol.* **23:**226–240

DeHaan, R.L., Chen, Y.-H. 1990. The role of gap junctions in embryonic development. *Ann. N.Y. Acad. Sci.* **588:**164–173

DeHaan, R.L., Chen, Y.-H., Penrod, R.L. 1989. Voltage-dependent junctional conductance in embryonic heart. *In:* Molecular and Cellular Mechanisms of Antiarrhythmic Agents. L. Hondeghem, editor. pp. 19–43. Futura, Mount Kisco (NY)

Dunlap, K., Takeda, K., Brehm, P. 1987. Activation of a calcium-dependent photoprotein by a chemical signalling through gap junctions. *Nature (London)* **325:**60–62

Ebihara, L., Beyer, E.C., Swenson, K.I., Paul, D.L., Goodenough, D.A. 1989. Cloning and expression of a *Xenopus* embryonic gap junction protein. *Science* **243:**1194–1195

Fraser, S.E., Green, C.R., Bode, H.R., Gilula, N.B. 1987. Selective disruption of gap junctional communication interferes with a patterning process in hydra. *Science* **237**:49–55

Fujii, S., Hirota, A., Kamino, K. 1981. Optical indications of pacemaker potential and rhythm generation in early embryonic chick heart. *J. Physiol. (London)* **312**:253–263

Gilula, N.B., Reeves, O.R., Steinbach, A. 1972. Metabolic coupling, ionic coupling and cell contacts. *Nature (London)* **235**:262–265

Green, C.R. 1988. Evidence mounts for the role of gap junctions during development. *Bioessays* **8**:7–10

Guthrie, S.C., Gilula, N.B. 1989. Gap junctional communication and development. *Trends Neurosci.* **12**:12–16

Harris, A.L., Spray, D.C., Bennett, M.V.L. 1981. Kinetics of a voltage-dependent junctional conductance. *J. Gen. Physiol.* **77**:95–117

Harris, A.L., Spray, D.C., Bennett, M.V.L. 1983. Control of intercellular communication by voltage dependence of gap junctional conductance. *J. Neurosci.* **3**:79–100

Hille, B. 1984. Ionic Channels of Excitable Membranes. Sinauer, Sunderland (MA)

Hobbie, L., Kingsley, D.M., Kozarsky, K.F., Jackman, R.W., Krieger, M. 1987. Restoration of LDL receptor activity in mutant cells by intercellular junctional communication. *Science* **235**:69–73

Imanaga, I., Kameyama, M., Irisawa, H. 1987. Cell-to-cell diffusion of fluorescent dyes in paired ventricular cells. *Am. J. Physiol.* **252**:*H*223–*H*232

Jack, J.J.B., Noble, D., Tsien, R.W. 1983. Electric Current Flow in Excitable Cells. pp. 225–228. Clarendon, Oxford

Jongsma, H.J., Wilders, R., van Ginneken, A.C.G., Rook, M.B. 1990. Modulatory effect of the transcellular electric field on gap-junction conductance. *In:* The Biophysics of Gap Junctions. C. Peracchia, editor. CRC, Boca Raton (FL) (*in press*)

Lawrence, T.S., Beers, W.H., Gilula, N.B. 1978. Transmission of hormonal stimulation by cell-to-cell communication. *Nature (London)* **272**:501–506

Lee, S., Gilula, N.B., Warner, A.E. 1987. Gap junctional communication and compaction during preimplantation stages of mouse development. *Cell* **51**:851–860

Lo, C.W., Gilula, N.B. 1979. Gap junctional communication in the post-implantation mouse embryo. *Cell* **18**:411–422

Loewenstein, W.R. 1979. Junctional intercellular communication and the control of growth. *Biochim. Biophys. Acta* **560**:1–65

Loewenstein, W.R. 1987. The cell-to-cell channels of gap junctions. *Cell* **48**:725–726

Mehta, P.P., Bertram, J.S., Loewenstein, W.R. 1986. Growth inhibition of transformed cells correlates with their junctional communication with normal cells. *Cell* **44**:187–196

Musil, L.S., Beyer, E.C., Goodenough, D.A. 1990. Expression of the gap junction protein connexin43 in embryonic chick lens: Molecular cloning, ultrastructural localization and post-translational phosphorylation. *J. Membrane Biol.* **116**:163–176

Rook, M.B., Jongsma, H.J., Van Ginneken, A.C.G. 1988. Properties of single gap junctional channels between isolated neonatal rat heart cells. *Am. J. Physiol.* **255**:H770–H782

Satin, J., Fujii, S., DeHaan, R.L. 1988. Development of cardiac beat rate in early chick embryos is regulated by regional cues. *Dev. Biol.* **129**:103–113

Schwartzmann, G., Wiegandt, H., Rose, B., Zimmerman, A., Ben-Haim, D., Loewenstein, W.R. 1981. Diameter of the cell-to-cell junctional membrane channels as probed with neutral molecules. *Science* **213**:551–553

Spray, D.C., Bennett, M.V.L. 1985. Physiology and pharmacology of gap junctions. *Annu. Rev. Physiol.* **47**:281–303

Spray, D.C., Harris, A.L., Bennett, M.V.L. 1981. Equilibrium properties of a voltage-dependent junctional conductance. *J. Gen. Physiol.* **77**:77–93

Stühmer, W., Conti, F., Suzuki, H., Wang, X., Noda, M., Yahagi, N., Kubo, H., Numa, S. 1989. Structural parts involved in activation and inactivation of the sodium channel. *Nature (London)* **339**:597–603

Vassilev, P., Scheuer, T., Catterall, W.A. 1989. Inhibition of inactivation of single sodium channels by a site-directed antibody. *Proc. Natl. Acad. Sci. USA* **86**:8147–8151

Veenstra, R.D. 1990*a*. Voltage-dependent gating of gap junction channels in embryonic chick ventricular cell pairs. *Am. J. Physiol.* **258**:C662–C672

Veenstra, R.D. 1990*b*. Voltage-dependent gating of gap junctional conductance in embryonic chick heart. *Ann. N.Y. Acad. Sci.* **588**:93–105

Veenstra, R.D. 1990*c*. Developmental changes in voltage-sensitivity of gap junctional conductance. *Biophys. J.* **57**:244*a*

Veenstra, R.D., DeHaan, R.L. 1986*a*. Electrotonic interactions between aggregates of chick embryo cardiac pacemaker cells. *Am. J. Physiol.* **250**:H453–H463

Veenstra, R.D., DeHaan, R.L. 1986*b*. Measurement of single channel currents from cardiac gap junctions. *Science* **233**:972–974

Veenstra, R.D., DeHaan, R.L. 1988. Cardiac gap junction channel activity in embryonic chick ventricle cells. *Am. J. Physiol.* **254**:H170–H180

Veenstra, R.D., DeHaan, R.L. 1989. Regulation of single channel activity in cardiac gap junctions. *In:* Cell Interactions and Gap Junctions. Vol. 2, pp. 65–83. N. Sperelakis and W.C. Cole, editors. CRC, Boca Raton (FL)

Warner, A. 1988. The gap junction. *J. Cell Science* **89**:1–7

Warner, A.E., Guthrie, S.C., Gilula, N.B. 1984. Antibodies to gap-junctional protein selectively disrupt junctional communication in the early amphibian embryo. *Nature (London)* **311**:127–131

Winkel, G.K., Nuccitelli, R. 1989. Large ionic currents leave the primitive streak of the 7.5 day mouse embryo. *Biol. Bull.* **176(S)**:110–117

Wolpert, L. 1978. Gap junctions: Channels for communication in development. *In:* Intercellular Junctions and Synapses. J. Feldman, N.B. Gilula, and J.D. Pitts, editors. pp. 81–96. Wiley, New York

Zhang, J.-T., Nicholson, B.J. 1989. Sequence and tissue distribution of a second protein of hepatic gap junctions, Cx26, as deduced from its cDNA. *J. Cell Biol.* **109**:3391–3401

Received 23 May 1990; revised 20 August 1990